Numerical Modeling of the Vortex/Airfoil Interaction

Argyris G. Panaras*
Defense Industries Directorate, Athens, Greece

A modeling of the vortex/airfoil interaction is presented, in which the finite-area of the real vortices is taken into consideration. Two vortex models are used. In the first, a disturbed piece of a vorticity layer is simulated by four rows of discrete vortices of small strength. In the second, a number of discrete vortices is arranged within a circle. The first model may simulate a shear layer or a wake and the second a well-formed vortex. The method has been applied to the calculation of the pressure induced on the surface of the airfoil by the interacting vortex. Both models yield similar results. It has been found that when the distance of the vortex from the surface of the airfoil is large, the finite-area of the vortex is not a significant factor in determining the induced pressure field. However, when the distance of the vortex from the surface is reduced, its shape is distorted and the induced-pressure pulses have lower amplitude than those induced by an equivalent point vortex. At the limit, where it impinges on the leading edge of the airfoil, the vortex is split in two and the time-dependent pressure coefficient takes on even negative values at some time intervals.

Nomenclature

a = radius of the basic transformation circle, Fig. 1
c = airfoil chord
C_L = lift coefficient
C_p = pressure coefficient
$f(\lambda)$ = transformation function of Joukofski airfoils
$F(\lambda)$ = complex potential of the flow
g = intermediate transformation plane, Fig. 1
h = transformation plane, Fig. 1
K = nondimensionalized vortex strength, Γ/aU_∞
l = length defined in Fig. 1
q = dynamic pressure
U_∞ = freestream velocity
u = horizontal velocity component
v = vertical velocity component
y = vertical coordinate
z = physical plane of the airfoil
α = absolute angle of attack
β = angle determining the camber of the airfoil, Fig. 1
Γ = circulation of the airfoil
λ = final plane of transformation of the airfoil, Fig. 1
ϕ = angle defined in Fig. 1
ω = apparent angle of attack

I. Introduction

THE interaction of vortices with airfoils is a phenomenon that appears in such applications as in the flow about a helicopter rotor, where the tip vortex may interact with the blade, and within the blades of turbomachines. Due to this interaction, aerodynamic noise is generated. In addition, the unsteady flow and, consequently, the aerodynamic forces may be considerably affected if the vortices pass very near the surface of the airfoils.

The forementioned effects have been demonstrated numerically by Srinivasan and McCroskey.[1] In their calculations of the unsteady transonic flowfield about an airfoil, they embedded a line vortex of given strength within a thin-layer Navier-Stokes solver. The path of the vortex develops as part of the solution. The concept of the line vortex has also been applied by Meier and Timm[2] to compare the trajectories of laboratory vortices about a symmetric airfoil, to solve with potential flow calculations, and to estimate far-field noise. Similar studies are also reviewed in Ref. 2.

However, the real vortices have a finite area. Thus, in any vortex/solid-body interaction, it is expected that during the convection of the vortex within the flowfield of the body its shape will be distorted and strained. The nearer the vortex passes by the surface of the body, the greater this distortion will be. In the limit, the vortex will be diffused within the boundary layer that envelops the body. Very clear evidence of this behavior has been provided by Rockwell and Knisely[3] for unsteady cavity flow. Similar behavior is expected in the vortex/airfoil interaction.

It seems very probable that the intensity of the dynamic effects caused by the presence of a vortex in an airfoil flowfield depends on the degree of distortion and straining of the vortex. In order to investigate this hypothesis, a mathematical model of the vortex/airfoil interaction is developed in the present paper, in which the finite-area character of the real vortices has been considered.

The technique of conformal transformations is applied to the case of a family of Joukofski airfoils. A finite number of discrete vortices is used for the simulation of the size of the interacting vortical structure. The term "discrete vortex" refers to a point vortex having a core radius sufficient to avoid the singular behavior that occurs when two vortices are in close proximity.

There are various ways to model the initial distribution of the discrete vortices. The simplest evolutionary model is the classical one of Rosenhead,[4] according to which a vortex sheet is represented by a number of point vortices distributed evenly along a sine wave. The time-dependent positions of the point vortices are estimated by application of the Biot-Savart law. Gradually, the sine wave is transformed into a vortical structure. Much better results are obtained if a finite thickness is given to the initial vortex sheet by specifying several rows of point vortices, each identical but with a small separation between the rows.[5] In this paper, the gradual transformation of a part of vortex sheet into a vortical structure will be studied in the presence of an airfoil, superimposing a uniform stream.

The assumption of a vortex of circular cross section, composed of a large number of point vortices, is an alternative model examined in this paper. In this model, it is assumed that the vortex has been formed far upstream of the airfoil and per-

Received Nov. 5, 1986, revision submitted April 28, 1986.

*Staff Engineer; presently National Research Council Research Associate, NASA Ames Research Center, Moffett Field, CA. Member AIAA.

mitted to convect within the flowfield of the airfoil. This model is near to the experimental data of Meier and Timm.[2]

In the applications of the present model, the vortex will start its trajectory from an initial point upstream of the airfoil. During its motion along the flowfield of the airfoil, its shape will be computed periodically, so that an overall picture of its evolution can be given. In addition, the induced pressure pulses on certain points of the airfoil will be calculated. These pressure pulses are useful in obtaining an impression of the noise field generated by the vortex/airfoil interaction. They also serve as a measure of the variation of the vortex strength caused by distortion of its shape. The degree of this variation may be obtained by comparing the pressure pulses associated with the finite-size vortex to the corresponding pulses induced by a point vortex of equal strength.

II. Description of the Model

According to the classical wing theory, a Joukofski airfoil may be obtained from the flow about a displaced circle by a single conformal transformation. Referring to Fig. 1, the following successive transformations transform the flow about the shown airfoil into the one about a line segment of the λ plane:

$$z = h + l^2/h \tag{1}$$

$$g = h - be^{i\phi} \tag{2}$$

$$\lambda = g + a^2/g \tag{3}$$

If it is assumed that the vortical structure is composed of N discrete vortices, each of strength Γ, then the complex velocity potential at a point λ in the transformed plane is

$$F(\lambda) = U_\infty \left(ge^{-i\omega} + \frac{1}{ge^{-i\omega}} \right) + \frac{i\Gamma}{2\pi} \sum_{n=1}^{N} \ell n(\lambda - \lambda_n) - \frac{i\Gamma}{2\pi} \sum_{n=1}^{N} \ell n(\lambda - \bar{\lambda}_n) \tag{4}$$

where ω is the apparent angle of attack.

The velocity field induced on a point z in the airfoil plane is given by

$$u(z) - iv(z) = \frac{dF}{d\lambda} \frac{1}{f'(\lambda)} = \left(\frac{g^2 e^{-i\omega} - e^{i\omega}}{g^2 - 1} + \frac{iK}{2\pi} \sum_{n=1}^{N} \frac{1}{\lambda - \lambda_n} - \frac{iK}{2\pi} \sum_{n=1}^{N} \frac{1}{\lambda - \bar{\lambda}_n} \right) \frac{1}{f'(\lambda)} \tag{5}$$

where $z = f(\lambda)$ is the transformation function. The velocities have been nondimensionalized by U_∞ and the lengths by the radius a of the basic circle, $K = \Gamma/U_\infty a$, and the derivative $f'(\lambda)$ is estimated from Eqs. (1-3) to be equal to:

$$f'(\lambda) = \frac{g^2 (h^2 - l^2)}{h^2 (g^2 - 1)} \tag{6}$$

The velocity components of Eq. (5) are used here to estimate the pressure pulses induced on the surface of the airfoil by the interacting vortical structure. In order to isolate the effect of the elementary discrete vortices from the local pressure field generated by the parallel flow, the following appropriate pressure coefficient is used[6]:

$$c_p = \frac{(p_\kappa - p_\infty) - (p - p_\infty)}{q_\infty} = (u^2 + v^2) - (u_\kappa^2 + v_\kappa^2) \tag{7}$$

where the velocity components u and v are estimated from Eq. (5) assuming that there are no vortices in the flow ($K = 0$) and the components u_κ and v_κ include the vortex terms.

For calculating the velocity of the convected discrete vortices, Routh's rule has to be used, leading to the following equation for a vortex located at a point z_j;

$$u_j - iv_j = \left(\frac{g_j^2 e^{-i\omega} - e^{i\omega}}{g_j^2 - 1} + \frac{iK}{2\pi} \sum_{\substack{n=1 \\ n \neq j}}^{N} \frac{1}{\lambda_j - \lambda_n} - \frac{iK}{2\pi} \sum_{n=1}^{N} \frac{1}{\lambda_j - \bar{\lambda}_n} \right) \frac{1}{f'(\lambda_j)} - \frac{iK}{4\pi} \frac{f''(\lambda_j)}{[f'(\lambda_j)]^2} \tag{8}$$

The ratio of the derivatives in Eq. (8) is easily estimated in a nondimensional form as

$$\frac{f''(\lambda_j)}{[f'(\lambda_j)]^2} = \frac{2h^4}{(h^2 - l^2)^2} \left[\frac{l^2}{h^3} - \frac{(h^2 - l^2)}{h^2 g (g^2 - 1)} \right] \tag{9}$$

In order to have finite velocity at the trailing edge of the airfoil, the Kutta condition has to be fulfilled. This is achieved by introducing the following potential function:

$$F(g) = \frac{i\Gamma}{2\pi} \ell n g \tag{10}$$

The velocity induced by this potential function in the airfoil plane is

$$u_{in}(z) - iv_{in}(z) = \frac{i\Gamma}{2\pi} \frac{h^2}{g(h^2 - l^2)} \tag{11}$$

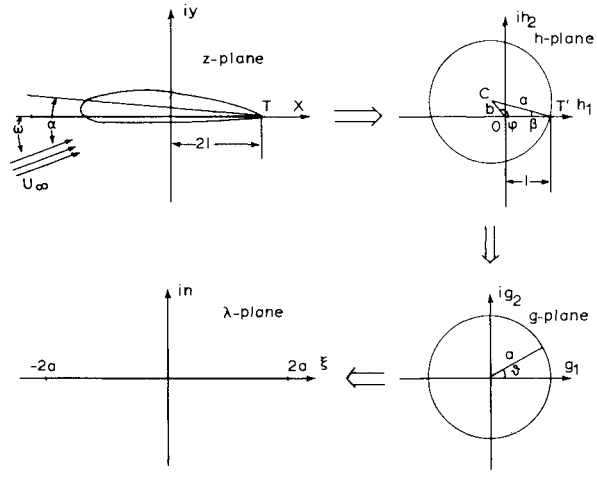

Fig. 1 Transformation of an airfoil into a line.

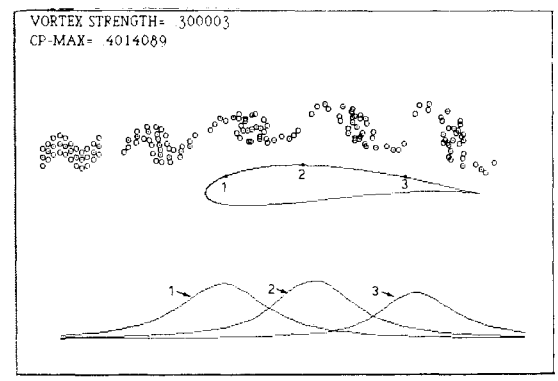

Fig. 2 Typical example of calculation.

The nondimensional circulation is given by: $\Gamma = 4n \sin\alpha$, where $\alpha = \beta + \omega$ is the absolute angle of attack. For each discrete vortex, this velocity is added to the one given by Eq. (8).

In the above formulation, only the steady Kutta condition has been satisfied. The unsteady Kutta condition requires vorticity to be shed from the trailing edge when the circulation about the airfoil is changing in time. The calculation of this vorticity may be easily included in an inviscid analysis like the present one. A detailed procedure is described by Huang and Chow.[8]

However, it seems that the small value of the strength of the vortices used in the present work and the fact that their vorticity is distributed rather than concentrated result in nonsignificant vorticity shedding. This will be clearly indicated later in Figs. 4b and 5b, in which the vortical elements will be seen to move very smoothly along the trailing-edge region of the airfoil surface, although only the steady Kutta condition has been satisfied. If the effect of the unsteady condition were strong, a departure from this tangential motion would have been observed.

III. Application of the Method

To apply the method described in the previous section, a family of Joukofski airfoils having a constant chord but variable zero angle-of-attack lift will be used. Referring to Fig. 1, the triangle (T'OC) is defined if the radius a, the length l, and the angle ϕ are known. If the length l is given, then the camber of the airfoil and, consequently, the zero angle-of-attack lift coefficient C_L depend on the value of the angle ϕ. The airfoils used have the characteristics shown in Table 1.

A typical example of calculation is shown in Fig. 2. The vortex model consists of one perturbed central row of clockwise discrete vortices and two external layers of passive tracers—i.e., vortices of zero strength. The tracers have been included to give a better impression of the evolution of the vortical structure. Various stages of development of the vortex are shown in Fig. 2. The disturbed vorticity layer is gradually transformed into a vortical structure that rotates in a clockwise direction. There is a strong similarity with the development of vortices from perturbed vortex sheets in an unbounded plane.[5] However, the formed structure is not smooth. It will be seen in Sec. III. A that better results are obtained if more rows of discrete vortices are used and if the total vorticity is distributed uniformly.

In Fig. 2, the numbered lines denote the corresponding value of the pressure coefficient [Eq. (7)] at the selected points 1-3 along the upper surface of the airfoil. Also, the maximum value of the pressure coefficient and the nondimensional strength of the vortex are given in Fig. 2. It is observed that the pressure coefficient at each point of the airfoil tends to zero when the vortex is far upstream or far downstream of it. As the vortex approaches a point, the pressure coefficient starts to rise, reaches its maximum value when it is near the point, and then gradually decays.

The value $k = 0.30$ has been assumed for the nondimensional vortex strength in most of the applications of this work. It has been estimated that, for this value, the pressure pulses induced on the surface of the airfoil, when the vortex is convected near the surface, have an amplitude of the same order of magnitude as the maximum suction generated by the freestream.

A. Effect of Interaction on Structure of Finite-Area Vortex

In this subsection, the models of finite-area vortices mentioned in the introduction will be applied to a typical configuration. For comparison, similar results based on calculations using the simpler model of a point vortex will be presented in each figure. Airfoil B will be used for these illustrations. The distance of an interacting vortex from the surface of the airfoil is one of the parameters that affect the

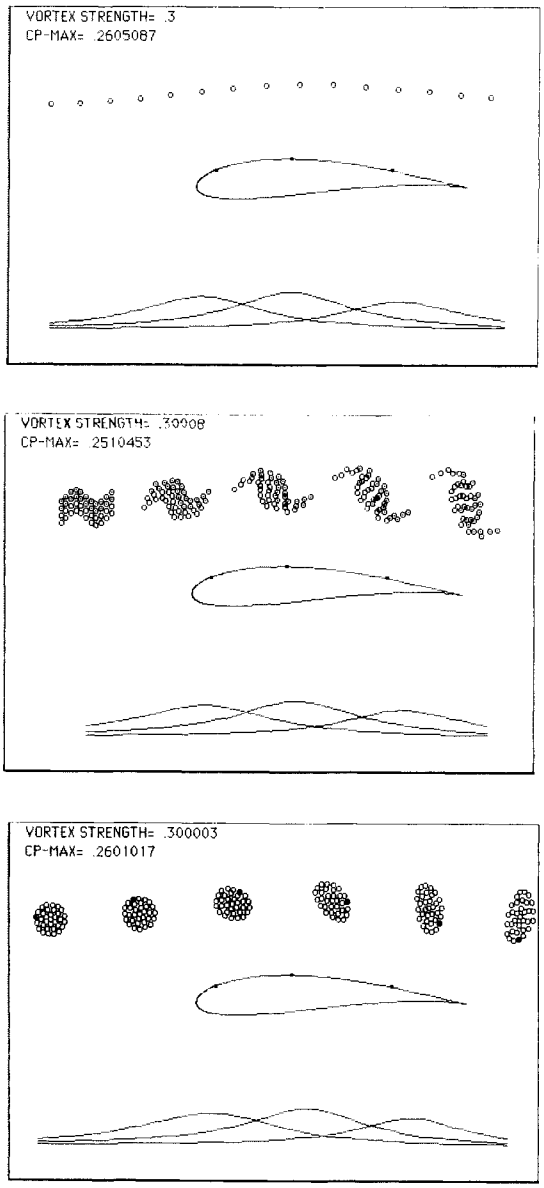

Fig. 3 Comparison of the vortex models: large distance from the airfoil.

Table 1 Airfoil characteristics

Airfoil	l	ϕ, rad	C_L
A	$0.9a$	2.00	1.14
B	$0.9a$	2.50	1.45
C	$0.9a$	3.14	0.0

distortion of the shape of the vortex and the intensity of the induced pressure pulses. To study the effect of distance on the vortex structure, three cases will be examined. In the first, the distance will be large ($y = 0.3c$) so that the effect of the flowfield on the shape of the vortex is very small. In the second case, the distance is very small ($y = 0.06c$), so that the vortex is subjected to a severe straining. In the third case, the vortex starts its convection along the airfoil axis ($y = 0$) and upon impinging on the leading edge is split into two.

The case of large distance of the vortex from the surface of the airfoil is shown in Fig. 3. In Fig. 3a, the small circles denote the trajectory of the point vortex. The vorticity-layer model is examined in Fig. 3b, in which four rows of discrete vortices are used to simulate the distributed vorticity layer. For a better illustration of the development of the vortical

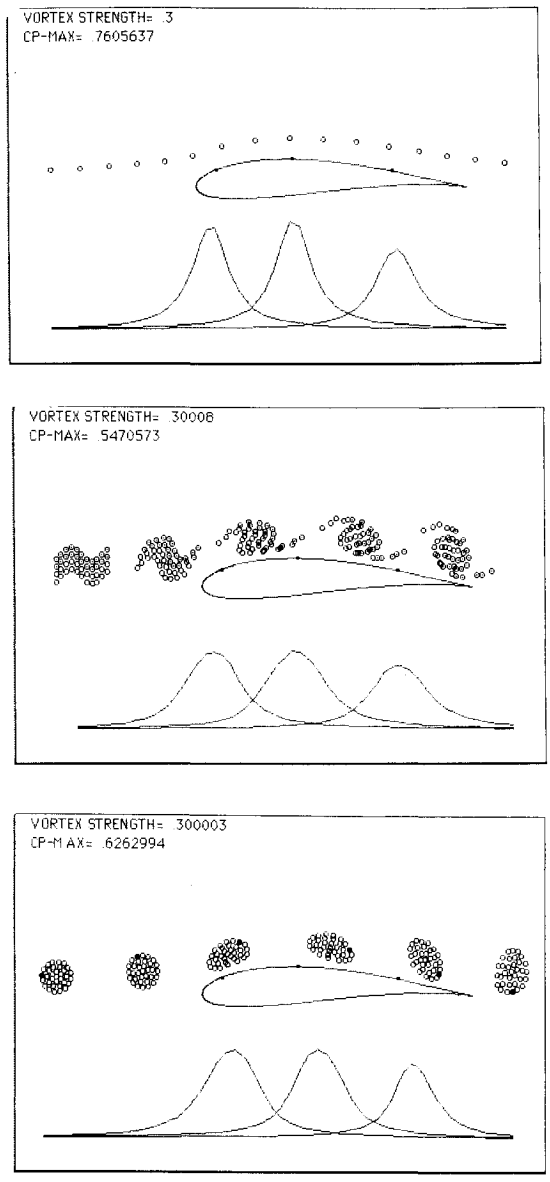

Fig. 4 Comparison of the vortex models: small distance from the airfoil.

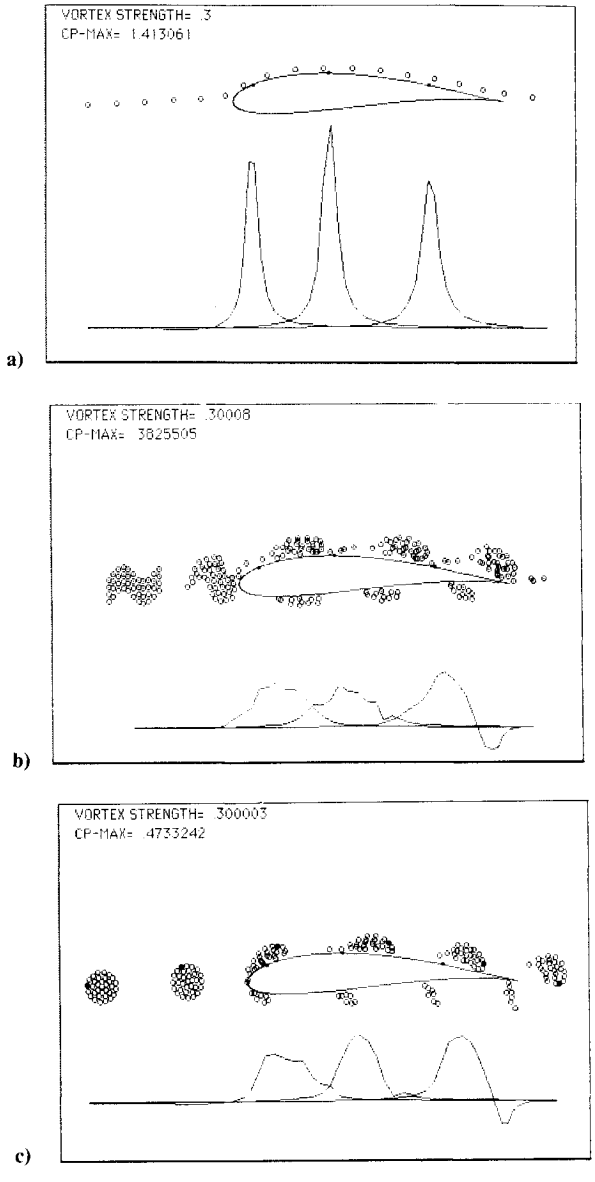

Fig. 5 Comparison of the vortex models: split of the vortex.

structure, different symbols have been used to denote the discrete vortices in each of the upper and lower two rows. All the discrete vortices have the same strength. The total strength of the vortical structure is equal to the standard value used in this paper. Also, the initial coordinates of the center of the vorticity layer coincide with the initial position of the point vortex. Thus, a comparison of the induced pressures is possible. The gradual development of the vortical structure is more evident here than in Fig. 2. The only difference between this case and that of the formation of a vortex in an unbounded plane is the observed elongation of the vortex when it passes over the region of the trailing edge of the airfoil. It will be shown in Sec. III. C that this elongation is due to the strain caused by the nonuniform airfoil field.

The circular cross-sectional model is applied in Fig. 3c. As previously mentioned, in this model it is assumed that the vortex has formed far upstream of the airfoil. The circular vortex of Fig. 3c consists of 33 discrete vortices of equal strength. The total strength of the vortex and the initial coordinates of the center of the circle are equal to the standard values of the previous figures. It is observed that, as the vortex is convected downstream, its size is enlarged, its shape gradually becomes elliptical, and it rotates as a whole about its own axis in a clockwise direction. A rotation of the elements of the vortex is also observed (illustrated by the rotation of the discrete vortex with the marked center).

The pressure pulses induced on the surface of the airfoil by the above two-dimensional vortex models (Figs. 3b and 3c) are quite similar to those induced by a discrete vortex (Fig. 3a). The maximum value and the shape of the pulses are both nearly identical. In view of this observation, it seems that, for relatively large distances of the vortical structure from the surface of the airfoil, the effect of its finite size on the induced pressure field is not significant.

The distance of the vortex from the surface of the airfoil has been reduced in Fig. 4. As expected from a consideration of the Biot-Savart law, the amplitude of the pressure pulses is increased, compared with those of Fig. 3. However, the observed differences between the pressure pulses induced by the discrete vortex (Fig. 4a) and by the two-dimensional vortex models (Figs. 4b and 4c) are the most significant observations in this figure. Not only has the value of the maximum pressure coefficient been reduced considerably, but the shape of the pressure pulses has become broader. Evidently, these differences are due to the effect of the two-dimensionality of the vortex and to its distortion as it approaches the surface of the airfoil. These effects are greatest in the case of the vorticity-layer model.

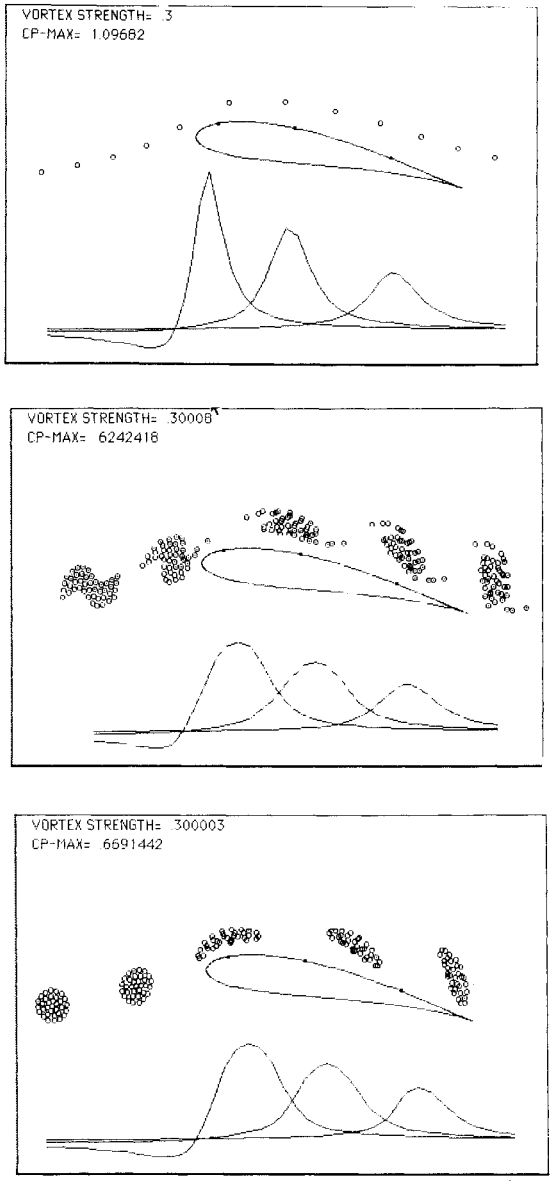

Fig. 6 Interaction at an angle of attack.

The extreme case of impingement of the vortex on the leading edge of the airfoil is shown in Fig. 5. In the case of the finite size models (Figs. 5b and 5c), the vortex is split into two and some of its elements slip along the lower surface of the airfoil. It is evident in this figure that the velocity of convection of the vortical elements is greater above of the airfoil than below of it. The effect of the two-dimensionality of the vorticies on the induced pressure field is really significant in this case. This figure demonstrates how erroneous the results of calculations based on the point-vortex model may be, if the distance of the vortex from the surface of the airfoil is very small. The realistic models of Figs. 5b and 5c give pressure pulses of amplitude less than one-third of the point vortex model. Even intervals of negative pressure are observed.

B. Effect of the Angle of Attack

In various practical applications, the airfoil is usually inclined to the stream. If a vortex is present in the flowfield, the higher the angle of attack, the greater the dynamic effects of its interaction with the airfoil will be, because the boundary layer formed on the upper side of the airfoil is more prone to separation at higher angles of attack. Thus, any overestimation of the pressure field induced on the surface of the airfoil by an interacting vortex may lead to the prediction of flow separation, while in reality the flow remains attached. Evidently, for a realistic estimation of the reduction of lift and the increase in drag, a realistic modeling of the vortex is necessary at high angles of attack.

An example of interaction similar to that presented in Fig. 4, but with the airfoil at an incidence ω of 10 deg is shown in Fig. 6. Again, the pressure pulses induced by the finite-area models are of much lower amplitude than the ones induced by

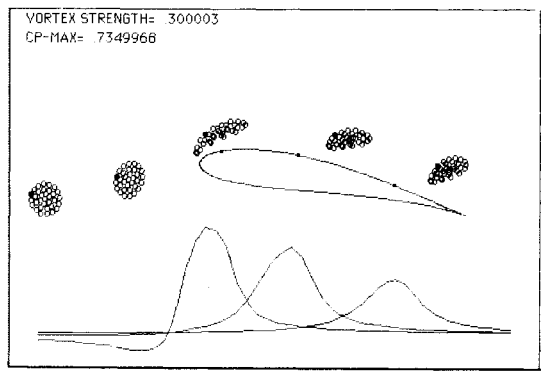

Fig. 7 Interaction with a simplified vortex model.

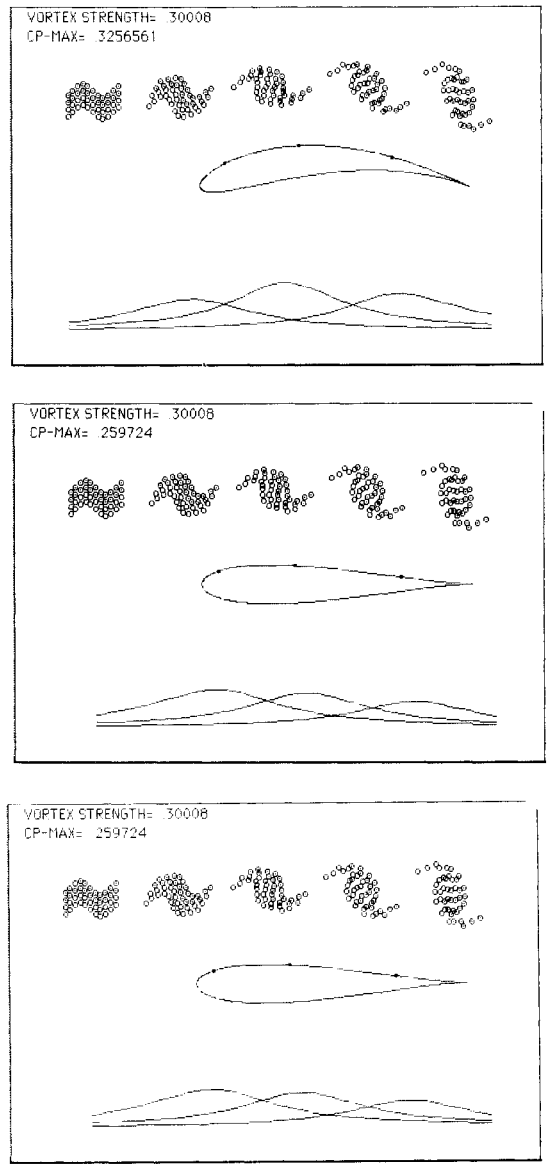

Fig. 8 Effect of the camber of the airfoil.

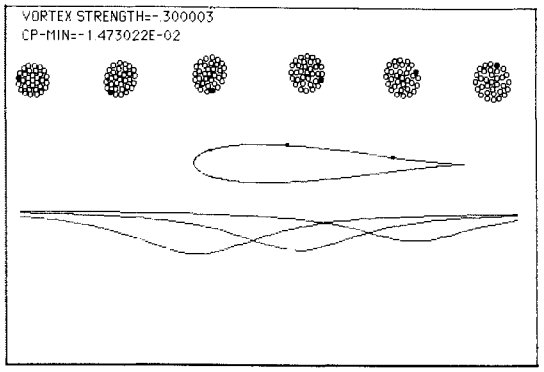

Fig. 9 Interaction with a counterclockwise vortex.

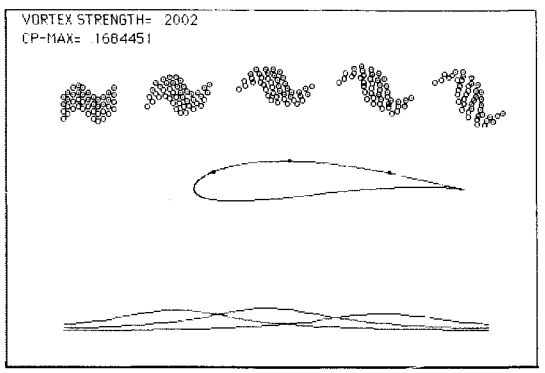

a)

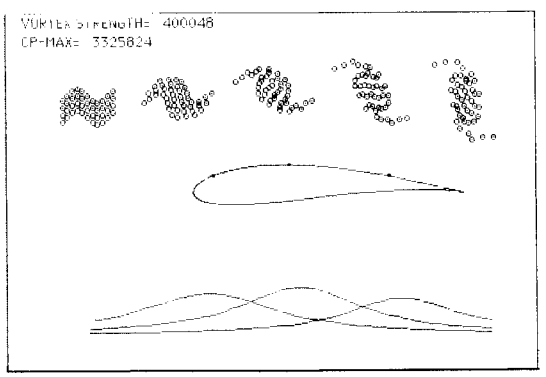

b)

Fig. 10 Effect of the vortex strength on the interaction.

the point vortex. Also, it is observed that the pressure pulses have much higher amplitude near the leading edge than near the trailing edge. Finally, the severe elongation of the vortical structures is a remarkable feature of the interaction at incidence.

In the course of this study, we tested a simplified version of the circular-section vortex model. In this version, the mutual interaction forces of the elementary discrete vortices were ignored. Thus, in this case, the changes of the shape of the vortical structure are due only to the effect of the airfoil flowfield and not to the internal forces of the vortex. Results of calculations similar to those of the regular circular-section vortex are shown in Fig. 7. The observed differences between these two versions are not significant. The deformation of the shape of the vortex and the intensity of the induced pressure pulses are similar. These results support the view that the simplified circular-section model may provide better results than the point-vortex model, if used in sophisticated calculation schemes, such as that of Srinivasan and McCroskey.[1] More examples of application of the simplified model are included in Ref. 7, where preliminary results of this study are reported.

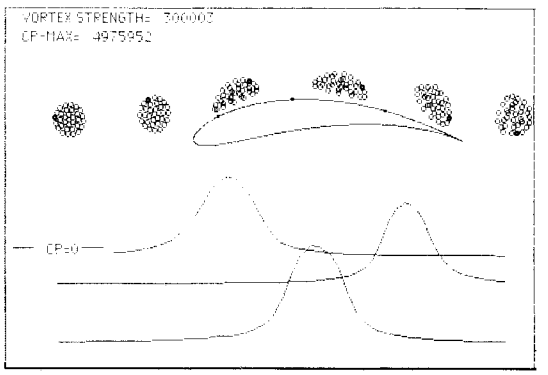

a)

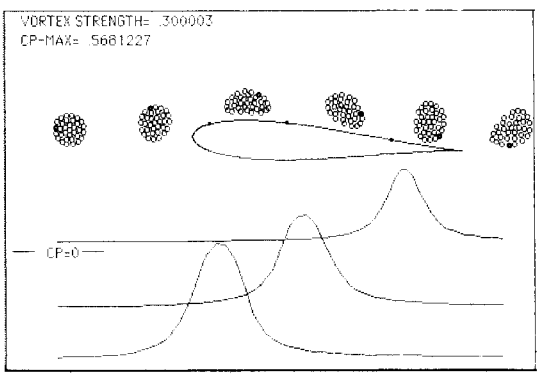

b)

Fig. 11 Examples of calculation considering the conventional pressure coefficient.

C. Effect of Camber of the Airfoil

To assess the effect on airfoil camber on the features of the interaction, calculations were performed with the airfoils A and C. Airfoil A is highly camber, while airfoil C is a symmetrical airfoil. Results of calculations based on the vorticity-layer model are shown in Fig. 8. In both cases, the initial distance of the vortex from the airfoil is equal to $y=0.3c$. It is observed that the gradual formation of the vortex is similar in both cases. However, the vertical elongation of the vortex near the trailing edge is much higher in the case of airfoil A (Fig. 8a) than in the case of airfoil C (Fig. 8b).

If a flat plate is used instead of an airfoil, no elongation of the vortex is observed. The vorticity layer is gradually transformed into a well-formed circular vortex that convects in the uniform flowfield (Fig. 8c). Thus, we may conclude that the elongation of a vortex within the flowfield of an airfoil is due to the strain caused by the variation of this field.

Concerning the effect of camber on the pressure pulses, it is seen that their amplitude is slightly higher for airfoil A. In addition, the maximum values in the symmetric airfoil appear in the region of the leading edge, while in the highly cambered airfoil they are shifted to its center.

IV. Discussion and Conclusions

In the present paper, the problem of appropriate simulation of a vortex/airfoil interaction has been addressed. The classical assumption of a point vortex is a useful tool for giving physical insight into many fluid dynamical phenomena. However, the fact is that real vortices have a finite area that cannot, in general, be ignored, especially when the trajectory of the vortex passes near an interacting surface.

To this end, two models of finite-area vortices have been examined. In the first, a piece of a vorticity layer consisting of a number of rows of discrete vortices of small strength is subjected to an initial perturbation by giving it a sine shape. During its motion, the layer is gradually transformed into a vortical structure. The shape of the vortical structure is affected

by the nonuniform flowfield. The distributed vorticity-layer model is appropriate for examining the interaction of airfoils with either shear layers or wakes. In the case of interaction with well-formed vortices, the second model that we have tested seems to be the more appropriate. This model consists of a number of discrete vortices arranged in a circular formation.

To our knowledge, the only existing experimental data on airfoil/vortex interaction are those of Meier and Timm.[2] These experiments were obtained by using a symmetrical airfoil and counterclockwise vortices. The conservation of the size and of the circular shape of the vortices is one remarkable feature of these experiments. Our model possesses this feature, if counterclockwise vortices are used. This is clearly shown in Fig. 9, where such a vortex structure has been used. It is also observed that the induced pressure pulses are negative. The comparison of our prediction with the experiments of Meier and Timm indicate that the circular-section model simulates the real vortices.

In addition to the examination of the development of the shape of a finite-area vortex, the pressure pulses induced at the surface of the airfoil by the vortex have been calculated. The results of these calculations provide a means for estimating the intensity of the dynamic effects of the vortex on the boundary layer.

The results of Secs. III. A and B indicate emphatically the necessity of considering the two-dimensional character of a vortex. More specifically, as long as a vortex passes above the surface of an airfoil at a great distance, the assumption of the single point vortex is a good approximation for estimating the induced pressure field. However, as this distance is decreased, a difference appears between the two-dimensional model and the point-vortex model. The nearer the vortex passes by the surface, the greater this difference becomes. In the limit, when the vortex impinges on the airfoil and is split in two, the actual pressure coefficient is of the order of one-third of the corresponding point-vortex model.

In all the applications, a standard value has been assumed for the strength of the interacting vortex ($k = 0.30$). Obviously, the amplitude of the induced pressure pulses depends on the value of the vortex strength. Furthermore, we have discovered that the spatial evolution of a vortical structure of given size also depends on the value of its strength. In order to illustrate these comments, Fig. 10 shows the typical case of Fig. 3b, but with a nondimensional vortex strength equal to $k = 0.2$ and 0.4. It is seen that, indeed, the formation of the vortical structure is delayed in the case of low strength, while it is accelerated in the case of high strength. Also, the amplitude of the pressure pulses is greater in the latter case.

All the figures in this paper represent a pressure coefficient that isolates the effect of the interacting vortex from the local flowfield. However, it is useful to give some examples of calculations using the conventional pressure coefficient. This is done in Fig. 11 for two typical interactions. For clarification, the level of the zero pressure is shown in these figures in addition to the maximum amplitude of the pressure curves.

To conclude, we hope that the present analysis has provided strong evidence of the need to consider the finite area of a vortical structure when algorithms are developed for treating the vortex/airfoil interaction. We also hope that this work will stimulate detailed experimental studies.

References

[1]Srinivasan, G. R. and McCroskey, W. J., "Numerical Simulation of the Interaction of Vortex with Stationary Airfoil in Transonic Flow," AIAA Paper 84-0254, 1984.

[2]Meier, G. E. A. and Timm, R. "Unsteady Vortex/Airfoil Interaction," *AGARD Conference on Unsteady Aerodynamics*, AGARD-CP-386, 1985.

[3]Rockwell, D. and Knisely, G., "The Organized Nature of Flow Impingement upon a Corner," *Journal of Fluid Mechanics,* Vol. 93, 1979, pp. 413-432.

[4]Rosenhead, L., "The Formation of Vortices from a Surface of Discontinuity," *Proceedings of the Royal Society of London,* Vol. A134, 1932, pp. 170-192.

[5]Acton, E., "The Modeling of Large Eddies in a Two-Dimensional Shear Layer," *Journal of Fluid Mechanics,* Vol. 76, 1976, pp. 561-592.

[6]Panaras, A. G., "Pressure Pulses Generated by the Interaction of a Discrete Vortex with an Edge," *Journal of Fluid Mechanics,* Vol. 154, 1985, pp. 445-462.

[7]Panaras, A. G., "Modeling of the Vortex/Airfoil Interaction," *AGARD Conference on Unsteady Aerodynamics,* AGARD-CP-386, 1985.

[8]Huang, M.-K. and Chow, C.-Y. "Trapping of a Free Vortex by Joukofski Airfoils," *AIAA Journal*, Vol. 20, March 1982, pp. 292-298.